Dependence of product formation from decomposition of nitroso-dithiols on the degree of nitrosation. Evidence that dinitroso-dithiothreitol acts solely as an nitric oxide releasing compound

Sonja Liebeskind,[a] Hans-Gert Korth,[b] Herbert de Groot[a] and Michael Kirsch*[a]

Received 29th January 2008, Accepted 31st March 2008
First published as an Advance Article on the web 7th May 2008
DOI: 10.1039/b801583j

Hitherto, the decay mechanisms of nitrosated dithiols as well as formation of related products have not been conclusively elucidated. In this paper, we demonstrate that nitrosated DL-dithiothreitol (DTT) decays *via* two independent pathways, that is, one producing exclusively nitric oxide and one producing (initially) nitroxyl ($HNO/^3NO^-$). The importance of the two decomposition pathways depends on the degree of nitrosation of DTT. Dinitroso-dithiothreitol (NODTTNO) generates quantitatively nitric oxide, whereas mononitroso-dithiothreitol (NODTT) yields initially nitroxyl. Since NODTT and DTT are both targets for nitroxyl, their availability governs the HNO-derived formation of nitric oxide (with NODTT as reactant) or hydroxyl amine and ammonium ion (with DTT as reactant). The formation of NH_4^+ from the HNO–DTT reaction probably proceeds by a stepwise, NH_2OH-independent mechanism, because DTT-derived sulfinamide was identified by N-15 NMR spectrometry as an intermediate. Our data are in line with the assumption that triplet nitroxyl ($^3NO^-$) is formed by a unimolecular decay of the deprotonated (thiolate) form of NODTT, because CBS-QB3 calculations predict the existence of a low-lying triplet state of the latter species. The identified pathways are proposed to be of general importance for physiological systems because control experiments showed that the physiological dithiol thioredoxin reacts in a similar manner.

Introduction

Nitric oxide (•NO), which is an important mediator in vasodilatation,[1] neurotransmission,[2] and immune reactions, is a short-lived intermediate in blood because it is rapidly trapped by the heme iron of hemoglobin. Therefore, it has been suggested that *in vivo* nitric oxide uses so-called "transporters" in order to prolong its life-time.[3] Thiols have been suggested to be involved in •NO transport, and protein-bound cysteine residues may regulate activities of a variety of enzymes after *S*-nitrosation in a fashion that parallels protein phosphorylation and dephosphorylation.[4,5] For instance, experimental evidence has been found that both exogenously and endogenously produced •NO impedes apoptosis *via* *S*-nitrosation of caspases.[6–8] One characteristic chemical feature of *S*-nitrosothiols is the transfer of the nitroso-function to another thiol ("transnitrosation"), reaction (1).

$$R^1SNO + R^2SH \leftrightarrows R^1SH + R^2SNO \quad (1)$$

By this reaction, low-molecular weight *S*-nitrosothiols can nitrosate cysteine residues in proteins. For instance, *S*-nitrosocysteine inhibits responses mediated by the *N*-methyl-D-aspartate subtype of the glutamate receptor of rat cortical neurons, presumably *via trans*-*S*-nitrosation of the channel.[9] Further, low-molecular weight RSNOs *trans*-*S*-nitrosate vital thiols in both skeletal and cardiac isoforms of the ryanodine receptor, which suggests that •NO modulates muscle activity.[10,11]

The *trans*-nitrosation reaction competes with the thiol-mediated reduction of the nitroso-function to NH_3 at excess thiol concentrations,[12] reaction (2).

$$2\ RSNO + 8\ RSH \rightarrow\rightarrow\rightarrow 5\ RSSR + 2\ H_2O + 2\ NH_3 \quad (2)$$

In addition, Wong *et al.*[13] reported that the reaction between thiols and *S*-nitrosothiols may yield nitroxyl (HNO), reaction (3),

$$R^1SNO + R^2SH \rightarrow R^1SSR^2 + HNO \quad (3)$$

which further produces •NO by reaction with a second molecule of *S*-nitrosothiol, reaction (4).

$$RSNO + HNO \rightarrow RSH + 2\ ^\bullet NO \quad (4)$$

However, the situation is less clear when the nitroso function is transferred to a dithiol in which the two thiol groups can interact with each other. The *S*-nitrosoglutathione (GSNO)-dependent nitrosation of the physiological dithiols dihydrolipoic acid (DHLA) and thioredoxin (Trxn) has been studied by several research groups, as overviewed by Stoyanovski *et al.*[14] However, conflicting reaction mechanisms have been proposed for this reaction (Scheme 1).

Arnelle and Stamler[15] reported that DHLA and the frequently used dithiol dithiothreitol (DTT) reduce GSNO to glutathione (GSH) and nitroxyl (HNO) *via* the intermediate formation of mononitroso-dihydrolipoic acid (**1** → **2** → **3**). This view was supported by data of Stoyanovsky *et al.*[14] On the contrary, Petit *et al.*[16] suggested that **2** decomposes to •NO and the

[a]*Institut für Physiologische Chemie, Universitätsklinikum Essen, Hufelandstrasse 55, 45122, Essen, Germany. E-mail: michael.kirsch@uni-duisburg-essen.de; Fax: +49 201-723 5943; Tel: +49 201-723 4108*
[b]*Institut für Organische Chemie, Universität Duisburg-Essen, Universitätsstrasse 5, 45117, Essen, Germany*

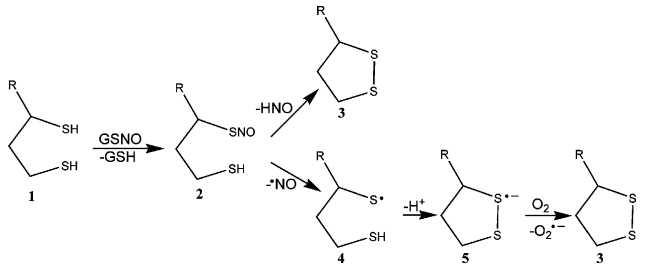

Scheme 1 Decomposition of mononitroso-dihydrolipoic acid according to Stoyanovski *et al.*[14]

S-centered radical **4**. The latter thiyl radical has been shown to undergo a rapid intramolecular ring closure to the radical anion **5**. Such radicals are known to react with oxygen at the diffusion-controlled limit to yield the superoxide radical anion ($O_2^{\bullet -}$).[17–19] Similar to the conversion **2** → **4**, Niktovic and Holmgren[19] reported that the key physiological dithiol thioredoxin (Trxn) catalyzes the denitrosation of GSNO with release of $^{\bullet}NO$ *via* the intermediate formation of mononitroso-thioredoxin (HS-Trxn-SNO). However, the occurence of reaction **2** → **4** is in question as *S*-nitrosothiols such as GSNO do not spontanously homolyze in the absence of any Cu^{2+}/Cu^{+}-ions.[20,21] Somewhat surprisingly, the suggestion of Wong *et al.*[13] that HNO releases $^{\bullet}NO$ from *S*-nitrosothiols *via* reaction (4) has not been taken into account for mononitrosated dithiols, although this reaction apparently explains the occurrence of both HNO and $^{\bullet}NO$.

In contrast to all the foregoing conclusions, Brock *et al.*[22] reported that *S,S′*-dinitrosated dithiols, but not mononitrosated ones, exhibited pharmacological effects typical for nitric oxide.

In physiological systems, clean mono- or dinitrosation of the available dithiols cannot be expected. From the above, it is obvious that the way in which the degree of nitrosation of the dithiols correlates with their chemical activity was unresolved so far. Therefore, we elucidated the chemical pathways of decomposition of nitrosated dithiols (see Scheme 2), using primarily DL-dithiothreitol as a model, in the absence and presence of certain targets, as a degree of nitrosation. These results are presented here. In contrast to all previous studies we clearly identify a HNO-dependent and a HNO-independent reaction channel of $^{\bullet}NO$ production. The HNO-independent pathway decisively involves the intermediacy of dinitroso-dithiols. The thermochemistry of all reactions is computationally established at the CBS-QB3 level of theory.

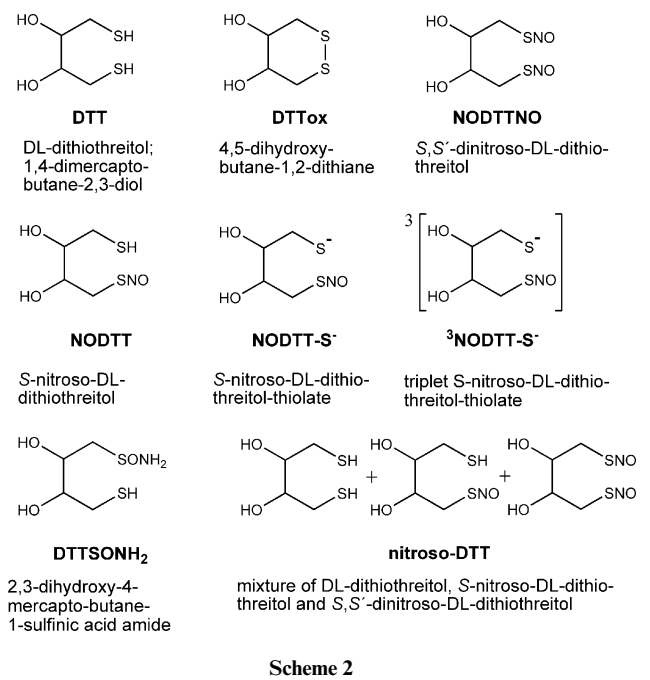

Scheme 2

Results

Mono- and dinitroso-DTT show very similar electronic absorptions at $\lambda_{max} = 332$ and 336 nm, respectively, with molar absorbtivities (NODTTNO: $\varepsilon_{336} = 1685\ M^{-1}\ cm^{-1}$, NODTT: $\varepsilon_{332} = 825\ M^{-1}\ cm^{-1}$) differing by about a factor of two.[23] The current literature does not give a conclusive answer to the question whether NODTTNO is only generated after complete mono-nitrosation of DTT because the nitrosation of the two thiol functions appears to proceed with the same rate constant.[23] Since quantum chemical calculations performed at the CBS-QB3 level of theory predicted both that the nitrosation of the second thiol group is a little more exergonic than the nitrosation of the first one and that the *trans*-nitrosation reaction between two NODTT molecules is additionally an exergonic reaction (reaction (5), Table 4, entry 5),

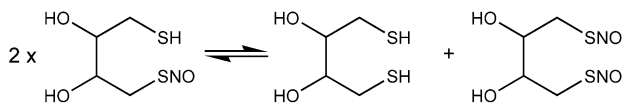

(5)

NODTTNO is expected to be present even in such nitroso-DTT solutions which were generated at a $[NO_2^-]/[DTT]$ ratio lower than 2.

Nitrosation was performed by reacting constant concentrations of DTT (60 μM) with varying amounts of sodium nitrite at pH 2 and rapidly adjusting the pH to 7.4 in order to slow down the spontaneous decomposition of nitrosated DTT. Since the decomposition at pH 7.4 is still relatively fast (see below), quantification of the yields of nitrosated species was not attempted, and the degree of nitrosation was expressed as the $[NO_2^-]/[DTT]$ ratio, assuming almost quantitative conversion of the minor reactant at all $[NO_2^-]/[DTT]$ ratios.

The validity of this assumption is demonstrated by Fig. 1A, showing an excellent linear dependence of the optical density at 336 nm on the $[NO_2^-]/[DTT]$ ratio, with a slope of 0.487 for $[NO_2^-]/[DTT]$ values ≤ 2. This would correspond to a nitrosation yield of 97.5 ± 1%. At $[NO_2^-]/[DTT]$ values ≥ 2, the optical density remained constant, clearly demonstrating that both thiol functions were essentially quantitatively nitrosated under the applied experimental conditions. The latter finding is in line with data of Brock *et al.*[22] Therefore, such solutions were generally applied for all further experiments.

The oxidation of dihydrorhodamine-123 (DHR-123) is, in the absence of catalytically active transition metals, a known test for the intermediacy of oxidizing nitrogen-oxide species.[24,25] From Fig. 1B it is understood that with increasing $[NO_2^-]/[DTT]$ ratio the oxidation of DHR-123 increased as well, until at $[NO_2^-]/[DTT] = 2$ a constant yield of rhodamine-123 is reached, *i.e.*, the same dependence as has been observed for the optical

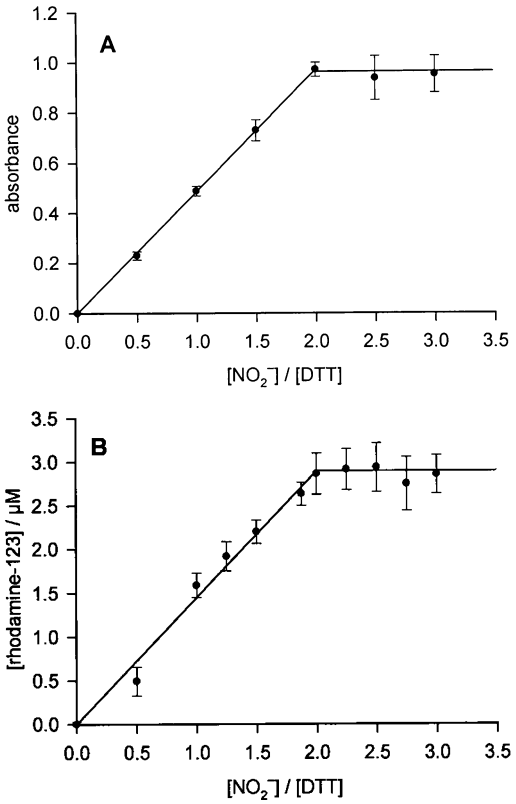

Fig. 1 Degree of DTT nitrosation. A: Dependence of the optical density at λ_{max} = 336 nm on the degree of DTT nitrosation expressed as $[NO_2^-]/[DTT]$ ratio. The absorbance was measured immediately after mixing the reactants ([DTT] = 60 μM) and adjusting the pH to 7.4 (T = 25 °C). B: Oxidation of dihydrorhodamine-123 as a function of DTT nitrosation expressed as $[NO_2^-]/[DTT]$ ratio. Mixtures of solutions of preformed nitroso-DTT (25 μM) and DHR-12 (50 μM) were allowed to react for 180 min at 37 °C.

density (Fig. 1A) is followed. This observation was somewhat unexpected, because hitherto it was generally believed that the reactive species responsible for oxidation of DHR-123 were exclusively released from NODTT.[14–16,19,26]

In order to verify a similar chemical activity of *in situ* nitrosated dithiols, the GSNO-mediated nitrosation of the primary aromatic diamine 4,5-diaminofluorescein (DAF-2) in the presence of DTT was studied (Fig. 2). Formation of the corresponding fluorescent triazole product DAF-2T indicates the intermediacy of •NO whose autoxidation in the presence of air produces the nitrosating species $^{\bullet}NO_2/N_2O_3$.

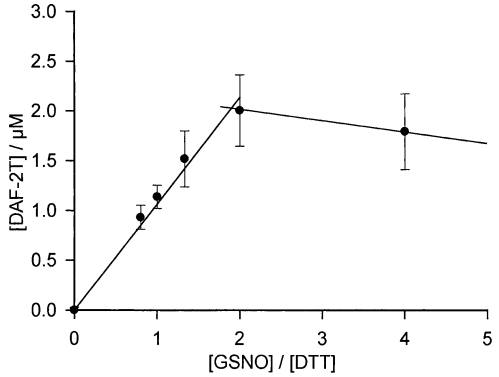

Fig. 2 Nitrosation of DAF-2 by *in situ* generated *S*-nitroso DTT. Mixtures of 60 μM GSNO and the corresponding concentration of DTT were allowed to react with 10 μM DAF-2 for 180 min at 37 °C in the dark.

In the absence of dithiol, GSNO is rather inefficient in converting DAF-2 to DAF-2T because only 0.14 ± 0.03 μM DAF-2T was detected. Since the nitric oxide-releasing decomposition of GSNO requires catalysis by transition metal ions (preferably copper and iron),[20] this low yield can be attributed to efficient complexation of traces of such metal ions by the added EDTA. Nitrosation of DAF-2 increased with increasing dithiol concentration, until a [GSNO]/[DTT] ratio of 2 is reached, that is, at the same ratio as was found from preformed nitroso-DTT (see Fig. 1). At higher [GSNO]/[DTT] ratios the fluorescence of DAF-2T decreased slightly, the reason for which was not further explored.

The foregoing observations strongly suggested that NODTTNO acts as a general nitrosating agent in the presence of oxygen. For further corroboration, the nitrosation of *N*-acetyltryptophan (NAT) by dinitroso-DTT was studied by H-1 NMR (Fig. 3).

Decomposition of NODTTNO was complete after a reaction period of 90 min (*vide infra*). The H-1 NMR spectrum then showed only the presence of *N*-nitroso-*N*-acetyltryptophan (NANT) and some residual NAT, thus clearly proving the capability of NODTTNO to nitrosate NAT.

In order to find evidence for the kind of the reactive intermediates which are responsible for the nitrosating/oxidizing capabilities of NODTTNO, the yields of products from reaction with NAT, melatonin, DAF-2, DHR-123, aminophenyl fluorescein (APF), and hydroxyphenyl fluorescein (HPF), respectively, were quantified (Table 1). Possible reactive intermediates for conversion of these targets as discussed in the literature are also listed.

Nitrosation of NAT, melatonin, and DAF-2 by NODTTNO proceeded uniformly with a yield of about 22%. It should be noted that all experiments were performed in phosphate buffer which is known to catalyse the hydrolysis of N_2O_3,[30] and this fact might

Table 1 Nitrosation/oxidation by dinitroso-dithiothreitol

Target	Substrate nitrosation/oxidation (%)	Possible intermediates	References
NAT	23.7 ± 7.5	N_2O_3, HNO	24,27
Melatonin	21.6 ± 1.5	N_2O_3, HNO	24,27
DAF-2	22.5 ± 0.6	N_2O_3, HNO	24,27
DHR-123	6.0 ± 0.3	$^{\bullet}NO_2$, HNO, ONOOH	25,28
APF	1.6 ± 0.1	HOCl, ONOOH	29
HPF	0.0 ± 0.0	$HO^{\bullet}$, $CO_3^{\bullet-}$	29

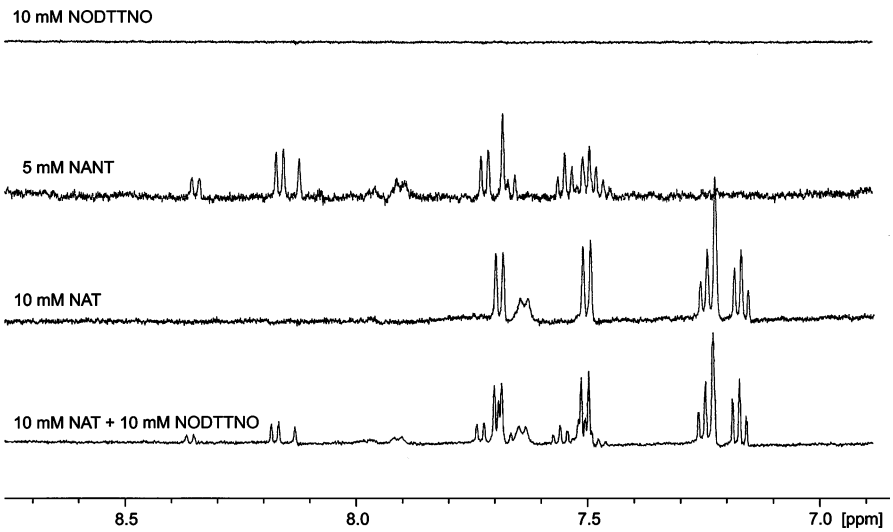

Fig. 3 H-1 NMR analysis. H-1 NMR (500-MHz) detection of nitrosation of *N*-acetyltryptophan (NAT) by NODTTNO (bottom). The spectrum (region of aromatic resonances) was recorded immediately after mixing of preformed NODTTNO (10 mM) and NAT (10 mM). Spectra of preformed NODTTNO (10 mM), *N*-nitroso-*N*-acetyltryptophan (NANT) (5 mM) and NAT (10 mM), respectively, are shown for comparison.

have limited the yields of the nitrosation products. Oxidation of DHR-123 and APF was significantly lower, and no oxidation was observed for HPF. APF and HPF are only converted to fluorescein by strongly oxidizing species like peroxynitrite and the hydroxyl radical. Since hydroxyl radicals can be generated from HNO,[31] the failure of NODTTNO to oxidize HPF disfavours the intermediacy of nitroxyl. Thus, the product yields of Table 1 strongly suggest the intermediacy of N_2O_3.

In order to discriminate whether NODTTNO nitrosates its targets *via* a reactive intermediate (N_2O_3) or directly by a bimolecular *trans*-nitrosation process, the influence of NAT on the decay of NODTTNO was monitored. The decay of NODTTNO was followed by reading its optical density photometrically at $\lambda =$ 545 nm in order to avoid interference with the formation of NANT ($\lambda_{max} = 335$ nm).

Inspection of Fig. 4 reveals that the decay of NODTTNO, with a half-life of about 2.4 min, is only slightly affected by the presence of NAT, even though NANT is produced (monitored photometrically at $\lambda_{max} = 335$ nm; data not shown). However, in the absence of NAT, the decay of NODTTNO does not follow a clean first-order rate law as evident from the logarithmic plot of the decay data. At longer reaction times, the decay of NODTTNO appears to be somewhat retarded, probably due to a second-order component. In fact, the best fit of the data points was obtained by assuming a superposition of a first-order and a second-order decay process. Noteworthy, in the presence of NAT, the decay of NODTTNO excellently followed a single first-order rate law with a rate constant of $k_1 = (4.91 \pm 0.07) \times 10^{-3}$ s^{-1} (298 K), corresponding to a half-life of 2.3 ± 0.1 min. The fact that in the presence of NAT, NODTTNO decays by a first-order process clearly indicates that the NODTTNO-mediated nitrosation of NAT proceeds *via* a reactive intermediate (*vide infra*), most reasonably N_2O_3. The intermediacy of N_2O_3 also would explain the retarded decay in the absence of NAT (Fig. 4) as N_2O_3 is known to catalyze the decay of mono-*S*-nitrosothiols.[32] The catalysis of decomposition of only one *S*-nitrosothiol group then inhibited the alternative (faster) decay, *i.e.*, the simultaneous bond breaking of the two RS–NO bonds in NODTTNO (see Discussion).

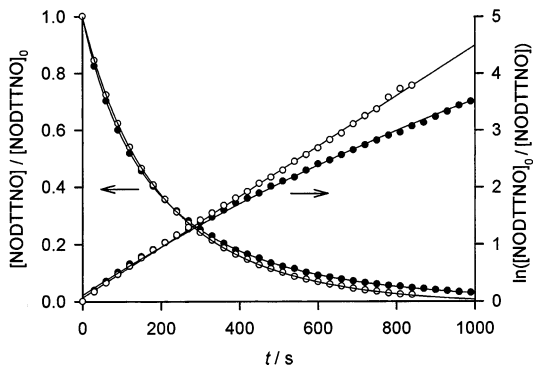

Fig. 4 Kinetics of NODTTNO decay. Decay of NODTTNO (2 mM) in the absence (closed circles) and in the presence (open circles) of *N*-acetyltryptophan (5 mM) at pH 7.4 ($T = 25$ °C). The optical density of NODTTNO was read at 545 nm. The solid lines through the left-hand data points are least-squares fits to a first-order rate law (open circles) and a linear combination of a first- and second-order rate law (closed circles).

Since NANT is highly effective in nitrosating thiols,[33] the decay of NODTT ($[NO_2^-]/[DTT] = 1$) was only measured in the absence of NAT. The decay of NODTT has been previously analyzed by Arnelle and Stamler[15] who reported a half-life of *ca.* 9 min at pH 7.4 and room temperature. We observed a moderately faster decay with a half-life of about 7 min at pH 7.4 and 25 °C (Fig. 5A). However, as evident from the regression line, the decay of NODTT is not of pure first-order. The decay was also dependent on the pH value, showing a maximum around pH 9 (Fig. 5B). This finding indicated that the decomposition of NODTT depended on the availability of the deprotonated thiol (thiolate) form. The increase of the half-life time at higher pH values is discussed below on the basis of a quantum-chemically supported mechanism.

In order to confirm the proposed release of HNO as the reactive intermediate from NODTT,[3] we applied a Mn^{III}–porphyrin

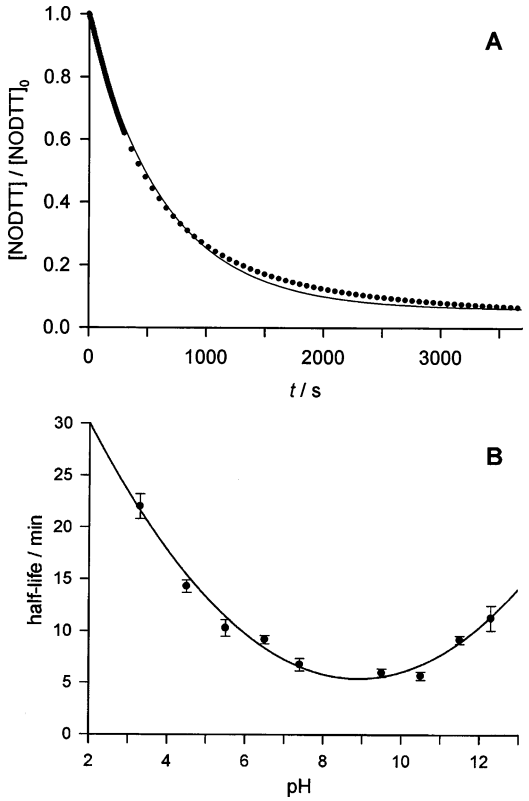

Fig. 5 Kinetics of NODTT decay. Decay of NODTT (2 mM, plus 100 μM EDTA) at 25 °C. A: Decay trace at pH 7.4. The optical density was monitored at λ_{max} = 336 nm. Solid line: least-squares fit to a first-order rate law. B: pH dependence of the half-life of NODTT (2 mM). The half-life values were estimated from simple first-order fits.

complex (manganese(III)-tetrakis(1-methyl-4-pyridyl)porphyrin pentachloride = Mn^{III}TMPyp) as a scavenger for nitroxyl as proposed by Marti *et al.*,[34] who used a related Mn^{III}–porphyrin derivative, manganese(III)*meso*-tetrakis-(*N*-ethylpyridinum-2-yl)-porphyrin, for the detection of nitroxyl. The HNO-trapping capability of Mn^{III}TMPyp was tested with the HNO donor Angeli's salt (AS). On addition of AS, the Soret band of Mn^{III}TMPyp (ε_{463} = 9.2×10^4 M^{-1} cm^{-1} [35]) decreased instantaneously with concomitant build-up of the absorption of the nitroso complex Mn^{II}TMPyp-NO at λ_{max} = 435 nm (ε_{435} = 1.1×10^5 M^{-1} cm^{-1} [36]) (Fig. 6A). Nitroso-DTT preparations at various $[NO_2^-]$/[DTT] ratios were analyzed.

In fact, an identical shift of the Soret band was observed in the presence of preformed nitroso-DTT synthesized at $[NO_2^-]$/[DTT] ratios of 0.25, 0.5, and 1 (Fig. 6B–D), which indicated the release of HNO during the decay of nitroso-DTT. Most remarkably, preformed NODTTNO did not cause any change of the 463-nm absorption (Fig. 6E). The production of HNO as a function of nitrosation of DTT (400 μM) was analyzed in more detail after a reaction period of 300 s (Fig. 6F). A constant amount of about 3.9 μM nitroxyl was trapped from $[NO_2^-]$/[DTT] ratios 0.75–1.25. The amount of trapped nitroxyl decreased to about 50% at a $[NO_2^-]$/[DTT] ratio of 1.5, and the Mn^{III}TMPyp assay failed to detect any nitroxyl at $[NO_2^-]$/[DTT] ratios $\geq$ 1.75. These data clearly demonstrate that the type of intermediate released from nitroso-DTT crucially depends on the level of nitrosation of DTT.

Although NODTTNO does not release any HNO during decomposition (Fig. 6E and F) but is nevertheless more reactive than NODTT (compare, *e.g.*, Fig. 1B), an intermediate other than nitroxyl has to be released. Petit *et al.*[16] claimed $^{\bullet}NO$ to be the main intermediate from decomposition of NODTT. Therefore, $^{\bullet}NO$ was measured polarographically from preformed and *in situ* generated nitroso-DTT, prepared at $[NO_2^-]$/[DTT] or [GSNO]/[DTT] ratios of 0.25–2. As the enzyme superoxide dismutase (SOD) is supposed to increase the yield of $^{\bullet}NO$ in the presence of HNO[37] as well as from $^{\bullet}NO/O_2^{\bullet-}$-releasing systems,[38] these experiments were performed in the absence and in the presence of SOD (100 units ml^{-1}). (Note that the foregoing experiments were carried out in an open experimental setup, thus only the equilibrium concentration of $^{\bullet}NO$ with respect to diffusion into the gas phase and autoxidation could be determined.)

As shown in Fig. 7, a maximum equilibrium concentration of $^{\bullet}NO$ of 12.4 μM was released from preformed nitroso-DTT synthesized at a $[NO_2^-]$/[DTT] ratio = 2. The $^{\bullet}NO$ equilibrium concentration decreased with decreasing $[NO_2^-]$/[DTT] ratio to about 50% at a ratio of 0.25. Noteworthy, at this ratio the presence of SOD increased the $^{\bullet}NO$ equilibrium concentration from 6.2 μM to 8.3 μM, thus indicating the intermediacy of either HNO or $O_2^{\bullet-}$. In order to discriminate between these two intermediates, the H_2O_2 concentration was measured in the absence and in the presence of SOD, because only a SOD-catalyzed dismutation of $O_2^{\bullet-}$ would lead to an increased level of H_2O_2. However, the H_2O_2 concentration in the presence of SOD (100 units ml^{-1}) (15.4 ± 1.6 μM) was within the error margins the same as in the absence of SOD (17.4 ± 0.7 μM). Thus, the SOD-mediated increase in the $^{\bullet}NO$ equilibrium concentration most likely derived from reaction with nitroxyl. The influence of SOD on the equilibrium $^{\bullet}NO$ concentration was even more pronounced when nitroso-DTT was *in situ* generated from the GSNO-DTT reaction, despite the fact that in this case the equilibrium concentration of nitric oxide was generally lower than from preformed nitroso-DTT (Fig. 7). These results further confirmed that both $^{\bullet}NO$ and HNO are released when DTT is only partially *S*-nitrosated.

To clarify whether a physiological dithiol can act in a similar manner, a few experiments were performed with nitroso-thioredoxin (nitroso-Trxn) (56.7 μM). Since preformed nitroso-Trxn cannot be synthesized at pH values lower than 4, it was synthesized at pH 5.4 by using an excess amount of NO_2^- (133.4 mM). Release of $^{\bullet}NO$ was initiated by adjusting the solution to pH 7.4. From such a solution, an equilibrium nitric oxide concentration of 2.9 ± 1.5 μM was determined, which corresponds to about 27% of the level that was achieved from DTT under the same conditions ($^{\bullet}NO$ production could not be detected in the absence of dithiol, thus ruling out inadvertent $^{\bullet}NO$ formation from nitrite *via* the HNO_2/N_2O_3 pathway). A similar relationship was found when the related nitroso-dithiols were generated *in situ* at pH 7.4 from the reaction of GSNO (250 μM) with Trxn or DTT (55.6 μM each). Here, the Trxn-dependent nitric oxide equilibrium concentration (1.21 ± 0.1 μM) amounted to 20% of that produced by DTT. Due to the presence of EDTA (100 μM), a GSNO-dependent $^{\bullet}NO$ release was not detected in the absence of dithiols. Thus, dinitroso-Trxn also releases nitric oxide at pH 7.4, although the yields and kinetics differ from that of DTT.

With respect to the suggested mechanism of HNO formation from mononitroso-dithiols (Scheme 1, reaction (2) → (3)), one

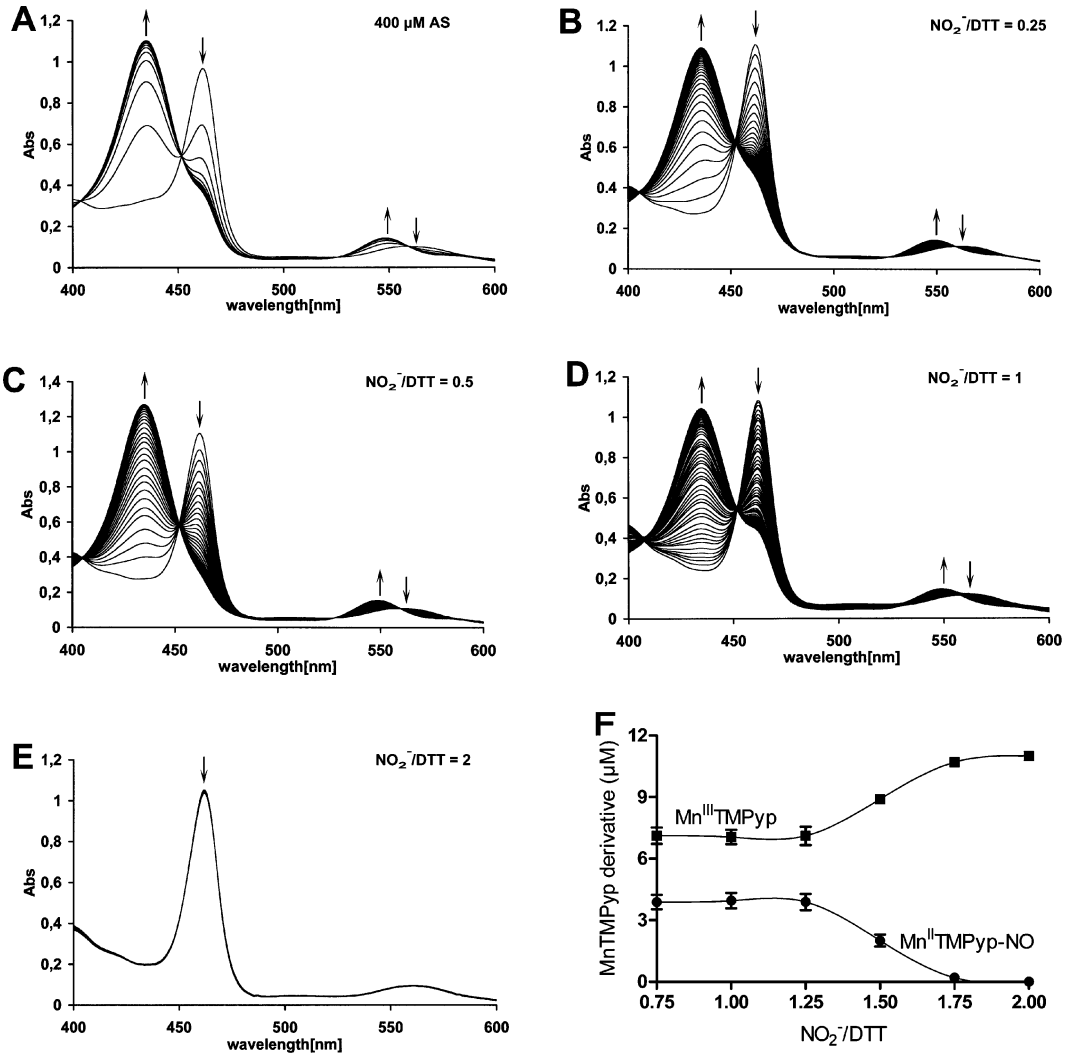

Fig. 6 Determination of HNO release from Angeli's salt and nitroso-DTT. A: Addition of AS (400 µM). B, C, D, E: Addition of preformed nitroso-DTT (500 µM) from various $[NO_2^-]$/[DTT] ratios (at a fixed NO_2-concentration). F: Amount of trapped nitroxyl after a reaction period of 90 s from preformed nitroso-DTT (500 µM) that were generated from various $[NO_2^-]$/[DTT] ratios (at a fixed NO_2^- concentration).

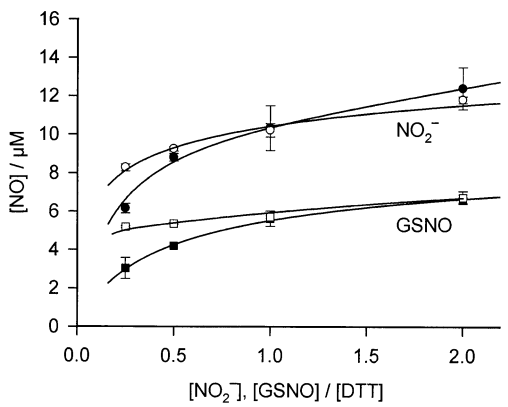

Fig. 7 Release of •NO. Equilibrium •NO production from preformed and *in situ* generated nitroso-DTT in the absence (closed symbols) and presence (open symbols) of SOD. Circles: Preformed ($[NO_2^-]$/[DTT]) nitroso-DTT (at a constant concentration of 250 µM SH groups). Squares: *In situ* generated nitroso-DTT from reaction of 250 µM GSNO with varying concentrations of DTT.

would expect that per mole released HNO one mole of thiol function is consumed. In order to check on this point, the concentration of the thiol functions of preformed nitroso-DTT prepared from various $[NO_2^-]$/[DTT] ratios (at a fixed amount of DTT) was quantified (Fig. 8).

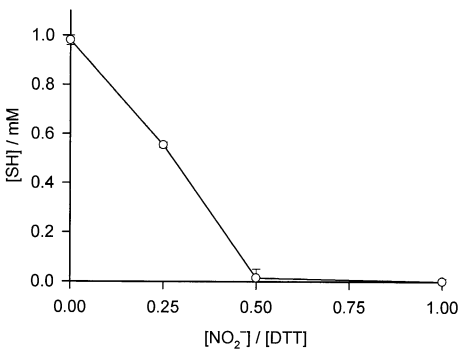

Fig. 8 Yields of thiol oxidation. Consumption of thiol functions of nitroso-DTT depending on the $[NO_2^-]$/[DTT] ratio.

In the absence of NO_2^-, 980 ± 20 μM thiol groups were found from 500 μM DTT 30 min after dissolution of DTT. This observation clearly demonstrates that DTT is not artificially consumed under our reaction conditions. In line with experiments described below and from literature data, all thiol functions were oxidized after complete decay of preformed nitroso-DTT prepared at $[NO_2^-]/[DTT]$ ratios ≥ 1. Surprisingly, however, about 98% of the thiol groups were already oxidized after decomposition of nitroso-DTT prepared at a $[NO_2^-]/[DTT]$ ratio of 0.5, *i.e.*, 986 ± 4 μM thiol were consumed by 250 μM NO_2^-, whereas a thiol depletion of only 500 μM had to be expected in the case of an exclusive HNO-producing pathway. A similar situation was observed for a $[NO_2^-]/[DTT]$ ratio of 0.25, because now 125 μM nitrite mediated the oxidation of 368 ± 11 μM thiol, instead of 250 μM theoretically. These observations made clear that the reaction mechanism is more complicated than hitherto assumed.[3,14,16] This further suggests that the enhanced oxidation of thiols may be accompanied by the release of a nitrogen species other than $^{\bullet}NO$ and HNO, respectively.

In order to identify the nitrogen products from preformed nitroso-DTT, N-15-enriched nitrite was applied at $[NO_2^-]/[DTT]$ ratios of 2, 1, 0.5, and 0.25, and the reaction mixtures were analyzed by N-15 NMR spectrometry after complete decomposition of nitroso-DTT (Fig. 9A–D).

From fully nitrosated DTT (NODTTNO; $[[N\text{-}15]NO_2^-]/[DTT] = 2$) only [N-15]nitrite ($\delta = 229$ ppm) and [N-15]nitrate ($\delta = -4.2$ ppm) were detected after decomposition at pH 7.4 (Fig. 9A). At $[[N\text{-}15]NO_2^-]/[DTT] = 1$, *viz.* NODTT, a prominent peak of $[N\text{-}15]NH_4^+$ ($\delta = -359.3$ ppm) was recorded in addition to $[N\text{-}15]NO_2^-$ and $[N\text{-}15]NO_3^-$. Neither typical HNO-derived decomposition products (N_2O, N_2) nor NH_2OH, a product expected from reduction of HNO by DTT,[15] could be detected (Fig. 9B). So far, NH_4^+ has not been reported as a product from decomposition of nitroso-dithiols, but it has been reported from reaction of GSNO with GSH.[12] At $[NO_2^-]/[DTT] = 0.5$, $[N\text{-}15]NH_4^+$ was the major product. Here, the yields of $[N\text{-}15]NO_2^-$ and $[N\text{-}15]NO_3^-$ were strongly diminished, but new signals of $[N\text{-}15]NH_2OH$ ($\delta = -277$ ppm) and a second, unknown product with $\delta = -300.8$ ppm were detected (Fig. 9C). Sulfinamides are characterized by N-15 NMR resonances around 300 ppm,[39] therefore, it was assumed that this resonance is due to the monosulfinamide of DTT ($DTTSONH_2$). In order to support this assumption, the N-15 NMR chemical shifts of $[N\text{-}15]DTTSONH_2$ and of the other products were quantum-chemically computed with the individual gauges for atoms in molecules (IGAIM) protocol at the B97-2/aug-cc-pVDZ level of theory. Since the reliability of the applied model to predict N-15 NMR resonances is not well reported in the literature, a small set of N-15 NMR resonances was selected as benchmark for comparing the IGAIM-B97-2/aug-cc-pVDZ method (Table 2).

The applied model predicted N-15 NMR resonances with a mean absolute deviation of 8.3 ppm and the N-15 chemical shift of $[N\text{-}15]DTTSONH_2$ is calculated to be 295.8 ppm, *i.e.*, 5 ppm lower than the N-15 NMR resonance of the unkonwn compound (Table 2). Thus, the calculations were not in conflict with the assignment of the resonance at −300.8 ppm to $[N\text{-}15]DTTSONH_2$. At a 4-fold excess of DTT, *i.e.* at $[[N\text{-}15]NO_2^-]/[DTT] = 0.25$ (Fig. 9D), only $[N\text{-}15]NH_2OH$ and $[N\text{-}15]NH_4^+$ were found as

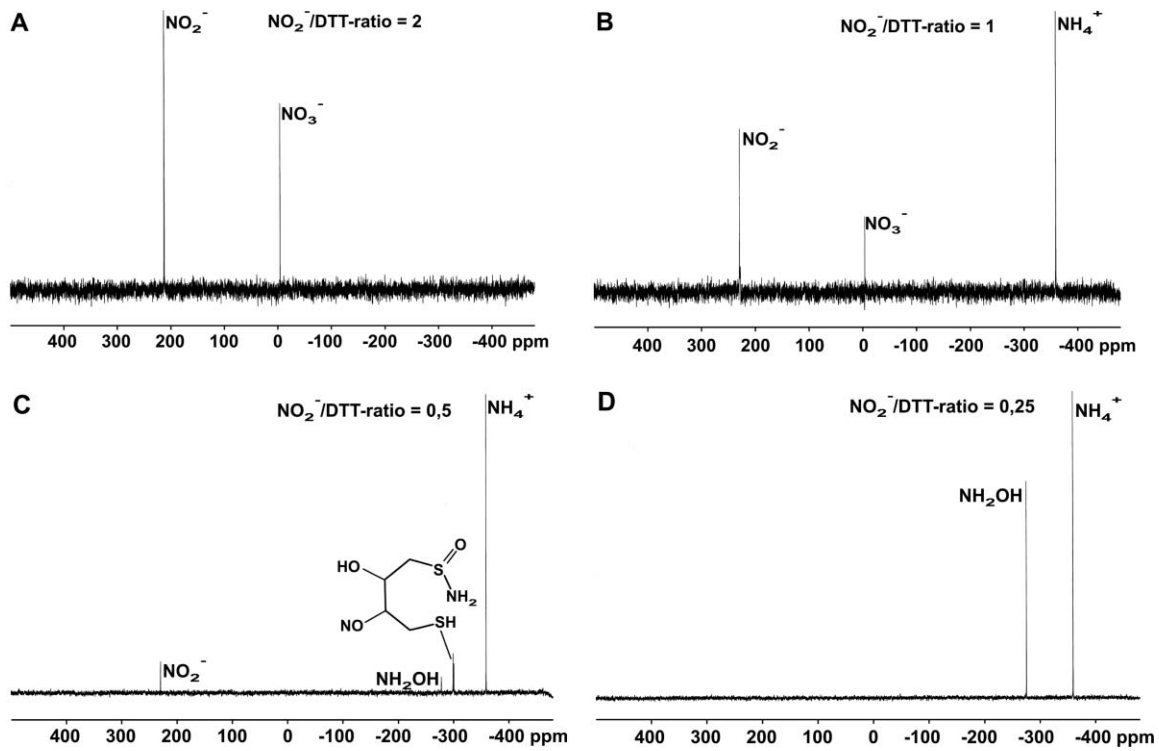

Fig. 9 N-15 NMR spectrometric product analysis of decomposed nitroso-DTT solutions. Preformed nitroso-DTT at various $[[N\text{-}15]NO_2^-]/[DTT]$ ratios (100 mM [N-15]nitrite, 100 μM EDTA, final pH = 7.4) were allowed to decompose for 6 h at room temperature. Chemical shifts (δ) are given in parts per million (ppm) relative to nitromethane ($\delta = 0$) as an external standard.

Table 2 Quantum-chemically calculated isotropic absolute shielding constants and N-15 chemical shifts (δ, in ppm)

	Isotropic shielding constant[a]	Isotropic chemical shift		
Compound	B97-2	B97-2	Exp.[40]	Deviation
[N-15] CH_3NO_2	−125.8	0.0	0.0	
[N-15]NO_2^-	−356.1	230.3	228.9	+1.4
[N-15]CH_3ONO	−334.4	208.6	184.0	+24.6
[N-15]$(CH_3)_2NNO$	−280.5	154.7	155.2	−0.5
[N-15]NO_3^-	−120.9	−4.9	−3.5	−1.4
[N-15]N_2	−55.3	−70.5	−69.6	−0.9
[N-15]CN^-	1.0	−126.8	−102.5	−24.3
[N-15][$^-$N=**N**$^+$=N$^-$]	2.7	−128.5	−131.5	+3.0
[N-15]CH_3CN	22.4	−148.2	−135.8	−12.4
[N-15]**N**NO	20.2	−145.9	−147.3	+1.3
[N-15]$(CH_3)_2$**N**NO	11.4	−137.2	−148.7	+11.5
[N-15]SCN^-	63.5	−189.3	−174.1	−15.2
[N-15]N**N**O	108.8	−234.6	−235.5	+0.9
[N-15]NH_2OH	150.1	−275.9	−278.1	+2.2
[N-15][$^-$N=N$^+$=**N**$^-$]	168.4	−294.2	−280.6	−13.6
[N-15]CH_3NCS	168.1	−293.9	−290.9	−3.0
[N-15]OCN^-	194.5	−320.3	−302.9	−17.4
[N-15]NH_4^+	241.5	−367.3	−359.6	−7.7
mean deviation				−3.0
mean abs. deviation				8.3
unknown			−300.8	
[N-15]$DTTSONH_2$	170.0	−295.8		

[a] Isotropic absolute shielding constants were calculated using the IGAIM protocol at the B97-2/aug-cc-pVDZ//B97-2/aug-cc-pVDZ level of theory. Solvation corrections (nitromethane for nitromethane, acetonitrile for acetonitrile and CH_3ONO, acetone for $(CH_3)_2NNO$ and CH_3NCS, none for NNO, H_2O for all others) with the CPCM solvation model were performed at the same level of theory.

products. In conclusion, the N-15 NMR spectra confirmed that the products from nitrosated DTT strongly depend on the degree of nitrosation of DTT, or, *vice versa*, the availability of free SH goups.

Since product yields are difficult to be quantified by N-15 NMR spectrometry, the foregoing experiments were repeated at much lower concentrations and three of the four products, namely NO_2^-, NO_3^-, and NH_4^+, were independently quantified (Fig. 10). Percentage yields are given relative to the concentration of the thiol groups.

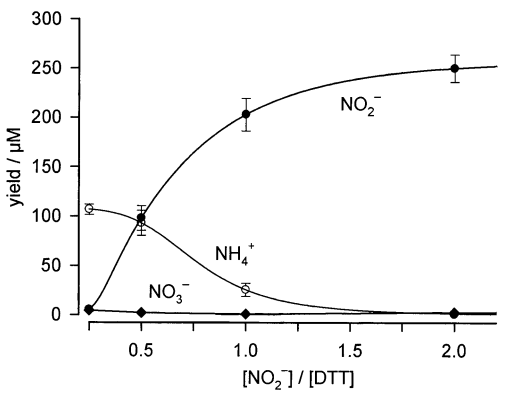

Fig. 10 Quantification of nitrite, nitrate, and ammonium from decomposed nitroso-DTT solutions. Nitroso-DTT prepared from various NO_2^-/DTT ratios (250 µM SNO function) was allowed to react for 3 h at 25 °C. Closed circles: NO_2^-, open circles: NH_4^+, closed diamonds: NO_3^-.

From NODTTNO ([NO_2^-]/[DTT] = 2) almost quantitative amounts of nitrite (248 ± 13 µM) were produced. With decreasing [NO_2^-]/[DTT] ratio, the yield of nitrite decreased continuously to about 2.1% at a [NO_2^-]/[DTT] ratio of 0.25. The yield of NH_4^+ changed inversely to the nitrite yield. About equimolar amounts (96 ± 12 µM) of nitrite and ammonium were produced at [NO_2^-]/[DTT] = 0.5, until the yield of NH_4^+ approached a limiting value of about 43% (107 µM) at [NO_2^-]/[DTT] ratios ≤ 0.25. Production of NO_3^- did not exceed 2% at any [NO_2^-]/[DTT] ratios. The observed changes of product yields paralleled those observed in the N-15 NMR experiments. According to the N-15 NMR spectra, the missing nitrogen content is due to formation of NH_2OH and $DTTSONH_2$ (see Fig. 9A–D,) which were not independently quantified. As NH_4^+ is formed from nitroso-DTT as long as unnitrosated DTT is available, the question arose whether NH_4^+ is formed from reaction of nitroso-DTT with DTT or from reduction of NH_2OH by DTT. In fact, in text books of inorganic chemistry it is mentioned that NH_2OH can be reduced to NH_4^+.

$$NH_2OH + 2\,e^- + 3\,H^+ \rightarrow NH_4^+ + H_2O \qquad (6)$$

As DTT is well known for its reducing capabilities, the yields of NH_4^+ from the NH_2OH–DTT reaction were determined by N-15 NMR spectrometry. Experiments were performed with solutions of [N-15]NH_2OH (200 mM) in the absence and in the presence of DTT (400 mM). In both cases, however, only the resonance of [N-15]NH_2OH was detected after a reaction period of 6 h, proving that the yield of [N-15]NH_4^+ must be lower than 3% with respect to the applied [N-15]NH_2OH concentration (spectra not shown). Another possibility of NH_4^+ formation would be the reduction of HNO by DTT. We therefore quantified the NH_4^+ production from the NH_2OH–DTT reaction as well as from the HNO–DTT reaction by means of the glutamate dehydrogenase assay (Table 3). Angeli's salt (250 µM) was employed as HNO source.

Table 3 Yield of ammonium ion from DTT reactions[a]

	NH_2OH + DTT[b]		AS + DTT[c]	
[NH_2OH]/[DTT], [AS]/[DTT]	Yield/μM	Yield (%)	Yield/μM	Yield (%)
0.25	22.7 ± 8.0	0.9	7.8 ± 1.0	3.1
0.5	19.0 ± 3.8	0.8	9.2 ± 2.1	3.7
1.0	40.2 ± 6.5	1.6	2.9 ± 1.8	1.2
2.0	39.4 ± 6.1	1.6	1.3 ± 1.8	0.5
No DTT	14.3 ± 2.2	0.6	1.0 ± 1.2	0.4

[a] Concentrations of NH_4^+ were quantified after a reaction period of 3 h (100 μM EDTA, $T = 37$ °C, pH 7.4). [b] 2.5 mM NH_2OH. [c] 250 μM AS.

In agreement with the above data, the production of NH_4^+ from the NH_2OH–DTT reaction did not exceed 2% with respect to the applied amount of NH_2OH. A slightly higher yield of approximately 3.5% was observed from the HNO–DTT reaction. Control experiments demonstrated that neither NH_2OH nor the decomposition products of Angeli's salt inhibited glutamate dehydrogenase at the applied concentrations (data not shown). Thus, neither the NH_2OH–DTT reaction nor the HNO–DTT one can explain the 43% yield of NH_4^+ from decomposition of nitroso-DTT in the presence of excess DTT, *i.e.* at [NO_2^-]/[DTT] = 0.25 (Fig. 9 and 10). Therefore, it must be concluded that NH_4^+ is formed *via* a pathway independent of the presence of HNO and NH_2OH, respectively.

In order to demonstrate that NH_4^+ may also be formed from an *in situ* generated nitroso-dithiol, additional experiments were performed with GSNO in the presence of Trxn and DTT, respectively. Under roughly physiological conditions (100 μM EDTA, pH 7.4, $T = 37$ °C), Trxn (170.8 μM) reacted with GSNO (341.6 μM) to give 20.7 ± 0.2 μM NH_4^+, about 20% of the amount that could be generated from DTT under the same conditions. Thus, NH_4^+ production cannot be ignored on decomposition of physiological nitroso-dithiols.

Discussion

In the present paper we proved for the first time that nitroso-dithiols decay through various independent pathways, the relative importance of which depends crucially on the degree of nitrosation. A fully dinitrosated dithiol yields solely nitric oxide as volatile product. Consequently, nitrite, formed *via* autoxidation of $^{\bullet}NO$[41,42] and subsequent hydrolysis of N_2O_3,[43] is essentially the only stable product (yield > 98%) in the presence of oxygen (Fig. 9). Although DTTox is the only detectable other product, it is not clear whether formation of $^{\bullet}NO$ from NODTTNO proceeds by simultaneous bond-breaking of the two RS–NO bonds in the dinitroso-dithiothreitol molecule (reaction (7)) or *via* a stepwise process (reaction (8)).

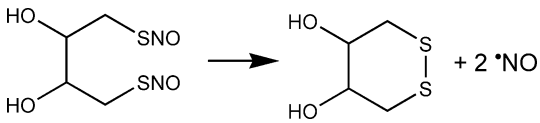

(7)

$$\text{NODTTNO} \rightarrow \text{NODTT}^{\bullet} + {}^{\bullet}\text{NO} \rightarrow \text{DTT} + 2\,{}^{\bullet}\text{NO} \qquad (8)$$

Quantum-chemical calculations performed at the CBS-QB3 level of theory predicted that reaction (7) is exergonic by −20.9 kcal mol^{-1} (Table 4, entry 1). The stepwise mechanism (reaction (8)) is predicted to proceed *via* a moderately endergonic reaction (21.8 kcal mol^{-1}, Table 4, entry 2) followed by a strongly exergonic one (−42.8 kcal mol^{-1}, Table 4, entry 3). The Gibbs free energy for homolytic bond dissociation of the S–NO function in NODTTNO is predicted to be 31 kcal mol^{-1}. This value is very similar to data experimentally observed for many simple mono-*S*-nitrosothiols.[44] Since the CBS-QB3 methodology is very reliable in predicting S–NO dissociation energies of *S*-nitrosothiols[45] and because such *S*-nitrosothiols do not spontaneously dissociate,[42] we doubt that the decomposition of NODTTNO proceeds *via* a stepwise homolytic dissociation mechanism. Nevertheless, a homolytic route cannot be ruled out with certainty.

Table 4 Quantum-chemically calculated Gibbs energies and aqueous solvation energies

Entry	Reaction[a]			$\Delta_r G_g$[b]/kcal mol^{-1}	$\Delta_r G_{solv}$[c]/kcal mol^{-1}	$\Delta_r G_{aq}$[d]/kcal mol^{-1}
1	NODTTNO	→	DTTox + 2 $^{\bullet}$NO	−21.5	0.6	−20.9
2	NODTTNO	→	NODTT-S$^{\bullet}$ + $^{\bullet}$NO	21.5	0.4	21.8
3	NODTT-S$^{\bullet}$	→	DTTox + $^{\bullet}$NO	−43.0	0.2	−42.8
4	NODTT + HNO	→	DTT + 2 $^{\bullet}$NO	−17.6	6.8	−10.7
5	2 NODTT	→	DTT + NODTTNO	−0.6	−2.8	−3.3
6	NODTT	→	DTTox + HNO	−9.0	−9.0	−18.0
7	NODTT-S$^-$	→	^{3}NODTT-S$^-$	6.0	7.1	13.1
8	NODTT	→	^{3}NODTT	29.4	−2.5	26.9
9	^{3}NODTT-S$^-$	→	DTTox + ^{3}NO$^-$	15.4	−37.8	−22.4
10	DTT + HNO	→	DTTox + NH_2OH	−24.9	−9.4	−34.2
11	NODTT + DTT	→	DTT-$SONH_2$ + DTTox	−50.1	−50.3	−100.4
12	DTT$SONH_2$ + DTT	→	2 DTTox + NH_3	−44.5	30.7	−13.7

[a] Thermodynamic properties were calculated using the complete basis set (CBS-QB3) methodology. [b] Gas phase data. [c] Solvation corrections from UHF/6-31+G(d)//CBS-QB3 single point calculations with the CPCM-UAHF solvation model for water.[44] [d] $\Delta_r G_{aq} = \Delta_r G_g + \Delta_r G_{solv}$.

In conclusion, the spontaneous release of nitric oxide from NODTTNO (and most likely of other dinitroso-dithiols) is a highly efficient, thermodynamically feasible process because the driving force of the reaction depends on a ring closure of a cyclic disulfide.

Now, the question arose why •NO release is still fairly good from nitroso-DTT solutions generated at $[NO_2^-]/[DTT]$ ratios ≤ 1, *i.e.* where mainly NODTT is formed and thus the release of HNO has to be expected (Fig. 6B–D). In this case, two processes for •NO production can be imagined: First, reaction of HNO with the parent *S*-nitrosothiol (reaction (4)) as proposed by Wong *et al.*[13] must be taken into account. In fact, the reaction of HNO with NODTT is predicted to be exergonic by 10.7 kcal mol^{-1} (Table 4, entry 4). Second, since *trans*-nitrosation between thiols and nitrosothiols is a well-known process,[42] NODTT might be in equilibrium with NODTTNO (reaction (5)), from which •NO is then released according to reaction (7) (Table 4, entry 1).

The fact that NODTT ($[NO_2^-]/[DTT] = 1$) did not decay by a clean first-order process (Fig. 5) would be in correspondence with reaction (5) because CBS-QB3 calculations predict that this reaction is slightly exergonic by 3.3 kcal mol^{-1} (Table 4, entry 5). However, in case of the physiological dithiol-thioredoxin, *trans*-nitrosation of its *S*-mononitrosated form (NOTrxn) analogous to reaction (5) appears unlikely due to high steric hindrance by the protein which would hamper exchange of the nitroso function to give *S*-dinitroso-Trxn. Since, however, ample •NO production from NOTrxn has been found, we conclude that •NO is primarily liberated from *S*-mononitrosothiols (in the absence of copper ions) *via* the HNO pathway (reaction (4)). Nevertheless, for sterically unhindered dithiols like DTT a contribution by reaction (5) cannot be ruled out.

Since reaction of HNO with the parent *S*-nitrosothiol is obviously the dominating pathway of •NO generation from mononitroso-dithiols, the question remained how HNO is released from NODTT. Although any details about the mechanism are missing in the literature, the reaction schemes given in those publications[14,15] suggest that generation of HNO from NODTT proceeds by direct, concerted elimination (reaction (9)).

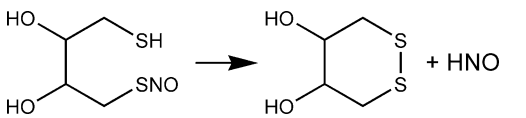

(9)

We were unable to locate a transition structure for reaction (9), so that the barrier height of the suggested elimination could not be calculated. The CBS-QB3 calculations predicted that the NODTT-dependent formation of HNO (reaction (10)) may be a proton-catalyzed process:

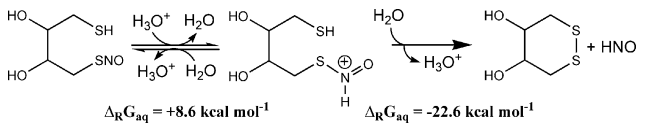

(10)

However neither direct elimination of HNO from the nitrosodithiol (reaction (9)) nor a proton-catalyzed process (reaction (10)) would explain the observed pH dependence of the decay rate of NODTT with a maximum (lowest half-life) at pH 9–10 (Fig. 5B). The pH dependence of Fig. 5B rather points to the deprotonated, thiolate form of NODTT (NODTT-S$^-$) as the reacting species. This would be in agreement with typical acidity constants of aliphatic thiols (compare, *e.g.* mercaptoethanol, $pK_a = 9.5$). Interestingly, our CBS-QB3 calculations predicted that only the thiolate anion of NODTT has a rather low-lying triplet state, about 13.1 kcal mol^{-1} above the singlet ground state (Table 4, entry 7). It is therefore proposed that the reaction may take place *via* a thermally accessible triplet state (reaction (11)), for which CBS-QB3 calculation predicts a driving force of −9.3 kcal mol^{-1} in aqueous solution (Table 4, entries 7 and 9).

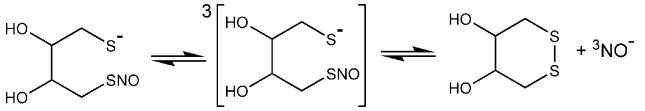

(11)

The possibility that NODTT-S$^-$ released alternatively $^1NO^-$ is unlikely because the experimentally determined singlet–triplet energy gap of the nitroxyl anion is −16.1 kcal mol^{-1},[46] so that reaction (11) would lose its negative driving force. The $^3NO^-$ anion comprises a unique conjugate acid–base couple (reaction (12)) with different ground-state multiplicities, preferring HNO formation at pH values lower than 11.4, the pK_a value of HNO.[47]

$$^3NO^- + H_3O^+ \rightleftharpoons HNO + H_2O \quad (12)$$

The fact that the half-life of NODTT again increased at pH > 10 (Fig. 5B) thus can be explained by the pK_a value of HNO and the reversibility of reaction (11). Since the spin inversion of NODTT-S$^-$ (reaction (11)) possesses a sizeable barrier of *ca.* 13 kcal mol^{-1}, one had to expect that bimolecular reactions (reactions (4) and (5)) could compete with reaction (11). The concentration of NODTT is governed by its self-reaction (reaction (5)) as well as by the HNO-mediated release of •NO (reaction (4)). At excess dithiol concentration, HNO is trapped by DTT and this reaction—as first discussed by Wong *et al.*[13] for the GSNO/GSH system—is the source of the observed products hydroxyl amine, sulfinamide, and ammonium ion. The formation of these compounds *via* the Wong *et al.* mechanism is also strongly supported by our CBS-QB3 calculations (Table 4, entries 10–12).

According to Singh *et al.*[12], the HNO-independent formation of NH_4^+ from GSNO *via* a stepwise mechanism with $GSNH_2$ as intermediate requires four equivalents of GSH. Such a mechanism cannot be ruled out with certainty. Nevertheless, the intermediacy of both HNO and the DTT-derived sulfinamide strongly supported the view that formation of NH_4^+ from decay of NODTT should primarily follow the Wong *et al.* mechanism. In conclusion, formation of all observed products is proposed to occur *via* the reactions summarized in Scheme 3.

Since the chemical properties of nitroso-DTT and nitroso-dihydrolipoic acid[3] on the one hand and of nitroso-DHLA and nitroso-Trxn[48] on the other hand are similar, we believe that the reactions outlined in Scheme 3 are quite general ones for the decay of nitroso-dithiols at physiological pH values. It has been suggested that Trxn reacts in the cytosol to yield either •NO[19] or NH_2OH.[48] In this work, experimental evidence is presented that the formation of the products depends on the degree of nitrosation of the dithiol. A low level of nitrosation means that the concentration of dinitroso-dithiol is negligibly low since

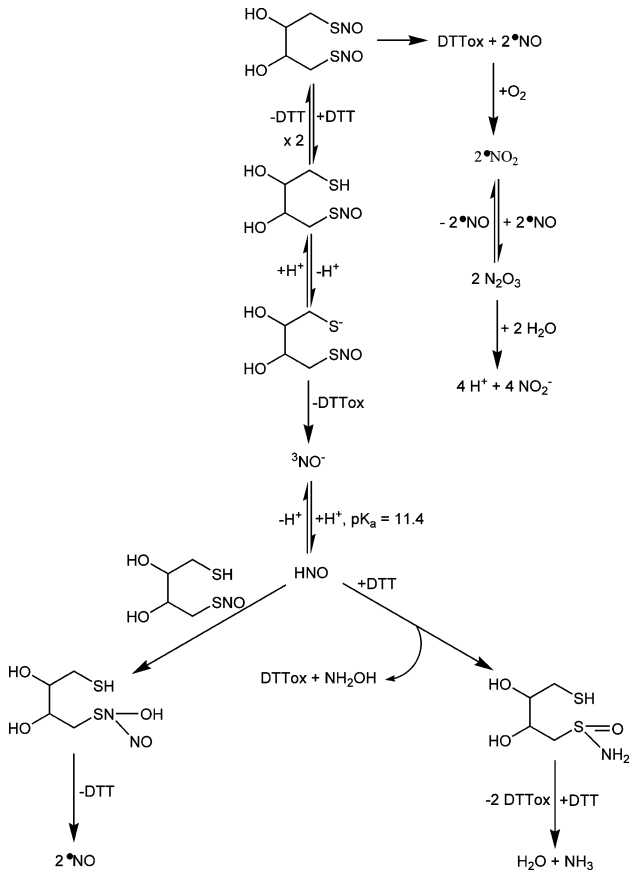

Scheme 3

reaction (5) is shifted to the left side. In intracellular milieu, the concentrations of RSNOs have been determined to be in the submicromolar range,[49] whereas that of Trxn and GSH are in the range of 5–50 μM[48] and 3–5 mM,[50] respectively. Under such conditions, the formation of the nitric oxide-yielding entity dinitroso-Trxn would be extremely low and only NH_2OH and NH_4^+ would be formed. The generation of NH_4^+ is favourable for biological systems as ammonium can be rapidly detoxified by many cell types *via* the urea cycle.[51] Thus, Trxn is expected to additionally act *in vivo* as a GSNO reductase but not as a GSNO-dependent nitric oxide synthase.

Experimental

Chemicals

Thioredoxin (*Escherichia coli*, purity ≥ 90%), *N*-acetyltryptophan (NAT), dithiothreitol (DTT), glutathione (GSH), Chelex 100, 5,5′-dithio-bis(2-nitrobenzoic acid) (DTNB) and L-glutamic dehydrogenase (GlDH) from bovine liver were obtained from Sigma (Hamburg, Germany). $Na[N\text{-}15]NO_2$ and $[N\text{-}15]NH_2OH$ labled with 99.3% N-15 were purchased from Aldrich/Isotech Inc (Hamburg, Germany). $NaNO_2$ and $(NH_4)_2SO_4$ were produced by Merck (Darmstadt, Germany). 4,5-Diaminofluorescein (DAF-2), diaminofluorescein-2T (DAF-2T), hydroxyphenyl fluorescein (HPF) and aminophenyl fluorescein (APF) were from Alexis (Grünberg, Germany). Angeli's salt (AS; purity ≥ 99%) and Mn(III)-tetrakis(1-methyl-4-pyridyl)porphyrin pentachloride (Mn(III)TMPyp) were obtained from Cayman Chemical (Michigan, US). All other chemicals were of the highest purity commercially available.

Experimental conditions

All experiments were carried out at 25 °C in 50 mM phosphate buffer (PB) if not described otherwise. Because nitrosation reactions are sensitive to the presence of metal ions,[42] solutions were treated with the chelating resin Chelex 100 prior to use as described previously,[52] and further supplemented with 100 μM EDTA.

Synthesis of nitrosated dithiothreitol

As previously described for other thiols,[53] 154.25 mg DTT were diluted in 50 mM PB containing 100 μM EDTA, and 69.0 mg $NaNO_2$ or 70.0 mg $Na[N\text{-}15]NO_2$ were diluted in doubly distilled water. Both solutions were mixed at the required ratio, and the synthesis was started by adding 1 M hydrochloric acid until a pH of 2 was attained. The reddish solutions were diluted immediately with 50 mM PB and 100 μM EDTA to give a 10-fold stock solution. The concentration was photometrically controlled (see Fig. 1). Samples were prepared as fast as possible because of the low half-life of nitroso-DTT[15] (see Results), and the pH was immediately adjusted to 7.4 with 1 M NaOH.

Synthesis of *S*-nitroso-glutathione

As described previously,[33] 3.07 g GSH and 0.69 mg $NaNO_2$ were allowed to react in a mixture of 20 ml purified water and 10 ml 1 M HCl for 40 min at 4 °C. Then, 20 ml acetone were added and the solution was stirred for another 10 min. The formed precipitate was filtered off, washed with 10 ml water, 3 times with 20 ml diethyl ether, dried in a desiccator and stored at −20 °C. The concentration of the prepared GSNO was quantified by reading the optical density at $\lambda_{max} = 545$ nm ($\varepsilon_{545} = 20\ M^{-1}\ cm^{-1}$).[54]

Synthesis of 1-nitroso-melatonin

1-Nitroso-melatonin (NOMela) was prepared as described by Kirsch and de Groot.[53] In brief, melatonin (232 mg) was dissolved in 4 ml acetone,10 ml water was added and the mixture stirred for several minutes. Afterwards 207 mg $NaNO_2$ and another 2 ml of water were added. 1.5 ml of 1 M HCl were added to the yellow liquid, shaken well and cooled to 1 °C. The mixture was extracted with 20 ml cold (1 °C) dichloromethane, and the separated organic phase dried with 750 mg Na_2SO_4. The solvent was evaporated at −20 °C, and the yellow solid was stored at −20 °C. The purity was determined photometrically at 345 nm ($\varepsilon_{345} = 7070\ M^{-1}\ cm^{-1}$).[53] To a 100-fold stock solution used for the experiments 20 vol% DMSO were added to prepare an aqueous solution of the lipophilic substance.

Synthesis of *N*-nitroso-*N*-acetyltryptophan (NANT)

The preparation of NANT as described by Bonnett and Holleyhead[55] was improved by Sonnenschein *et al.*[33] In brief, 526 mg NAT and 162 mg $NaNO_2$ were stirred in 20 ml purified water for 2 h at room temperature in the dark. The yellow mixture was cooled to 1 °C, and 10 ml of cold (1 °C) 1 M HCl were added. The yellow precipitate was immediately extracted with 60 ml ethyl acetate (1 °C). The organic layer was separated, and the

solvent evaporated at room temperature under reduced pressure (18 Torr) to yield 500 mg of NANT. The concentration of NANT was photometrically controlled with a SPECTROCORD S 100 spetrometer from Analytic Jena ($\varepsilon_{335} = 6100$ M^{-1} cm^{-1}).[55]

H-1 NMR spectrometric measurements

Solutions of 10 mM NODTTNO plus 10 mM NAT, 10 mM NODTTNO, 10 mM NAT, and 5 mM NANT, respectively, were prepared in 50 mM PB with 10% D_2O and 100 μM EDTA at pH 7.4. Spectra were recorded by 500 MHz H-1 NMR on a Bruker AVANCE DRX 500 instrument 90 min after sample preparation. Chemical shifts (δ) are given in parts per million (ppm) relative to tetramethyl silane ($\delta = 0$) as an external standard.

N-15 NMR identification of adducts

After incubation for 6 h at room temperature, sample aliquots were supplemented with 10% D_2O and analyzed by N-15 NMR spectrometry. The products were identified by 50.67 MHz N-15 NMR on a Bruker AVANCE DRX 500 instrument. Chemical shifts (δ) are given in parts per million (ppm) relative to neat nitromethane ($\delta = 0$) as an external standard.

Quantification of •NO

Release of nitric oxide was detected polarographically with a graphite nitric oxide-sensing electrode (World Precision Instruments, Berlin, Germany) immediately after sample preparation.

Quantification of dithiothreitol

The concentration of thiol functions of DTT was quantified as described by Ellmann and improved by us.[56] DTNB (39.6 mg) was dissolved in 50 mM PB (10 ml, pH = 7.0). The samples were diluted 10-fold with 100 mM PB (pH = 7.0) and to 1 ml of the diluted sample 6.67 μl stock solution of DTNB were added. The optical density of the formed *p*-nitrothiophenol anion ($\varepsilon_{412} = 13\,600$ M^{-1} cm^{-1})[57] was read photometrically after incubation for 20 min at room temperature. The test was calibrated with a solution of neat DTT.

Quantification of nitrite

Nitrite was quantified by using the Griess-reagent (0.1% naphthylethylendiamine-dichloride [Sigma] + 1% sulfanil-amide [Sigma] in 5% H_3PO_4).[58] At the given time of reaction, the samples were diluted 30-fold with 50 mM PB (pH = 7.5), afterwards a 2.5-fold volume of Griess-reagent was added. After 10 min of incubation at room temperature, the optical density was photometrically read at 542 nm. Calibration was carried out with a photometrically controlled solution of neat $NaNO_2$ ($\varepsilon_{354} = 22.9$ M^{-1} cm^{-1}).[58]

Quantification of nitrate

The concentration of nitrate was determined by a commercially available Nitrate-Test-Kit (Boeringer Mannheim/R-Biopharm, Germany) improved by us. In brief, nitrate is reduced by nicotinamide-adenine dinucleotide phosphate (NADPH) to nitrite in the presence of the enzyme nitrate reductase. To the samples, which were incubated for 20 min at room temperature, pyruvate and LDH were added, and the samples were incubated for another 20 min at room temperature. The total nitrite-concentration was determined by using the Griess-reagent as described above. The base level of nitrite was directly quantified from a similarly treated sample in the absence of nitrite reductase. The test was calibrated with a solution of neat $NaNO_3$, whose purity was controlled photometrically ($\varepsilon_{302} = 10$ M^{-1} cm^{-1}).[58]

Quantification of dihydroperoxide

Hydrogen peroxide was determined by the horseradish peroxidase-catalysed reaction of H_2O_2 with 4-amino-antipyrine and 3,5-dichloro-2-hydroxyl-benzenesulfonic acid. The pink-coloured product was measured photometrically at 513 nm.[59] Samples of nitroso-DTT having reacted 10 min in the absence and presence of SOD (100 units/ml) were measured after another 10 min of incubation at room temperature. Standard buffer solutuons of H_2O_2 were used for calibration.

Quantification of ammonium

The concentration of NH_4^+ was determined as described by Bergmeyer *et al*.[58] Samples were incubated at room temperature for 3 h, then, aliquots were diluted 2.48-fold with 1 M triethanolamine buffer (TEA, pH = 8.0). To this mixture were added 2.8 mM α-ketoglutarate, 177 μM NADH, and 0.8% glycerine. After incubation for 20 min at room temperature, optical density of the samples was read photometrically at 340 nm. Then, 7.2 units ml^{-1} L-glutamic dehydrogenase (GlDH) were added and the samples were incubated for another 20 min at room temperature. Finally, the optical density at 340 nm was read to calculate the decay of NADH ($\varepsilon_{340} = 6200$ M^{-1} cm^{-1}),[58] which is directly proportional to the concentration of NH_4^+. The test was calibrated with a solution of neat $(NH_4)_2SO_4$.

Qualitative detection of nitroxyl

HNO was determined as described by Marti *et al.*[34] for a related Mn(III)–porphyrin complex. To the prepared samples were added 10 μM of Mn(III)TMPyp. Aliquots were immediately photometrically measured by a SPECTROCORD S 100 spetrometer from Analytic Jena. On reaction with HNO, the Soret-band of Mn(III)TMPyp at 463 nm ($\varepsilon_{463} = 9.2 \times 10^4$ M^{-1} cm^{-1};[35]) decreased and that of Mn(II)TMPyp-NO at 435 nm ($\varepsilon_{435} = 1.1 \times 10^5$ M^{-1} cm^{-1};[36]) increased.

Determination of reactive intermediates from NODTTNO

NAT or melatonin (10 mM each, 50 mM PB, 100 μM EDTA, 20% DMSO, pH = 7.4, room temperature) were allowed to react with preformed NODTTNO (10 mM) for 90 min and the concentration of either NANT ($\varepsilon_{335} = 6100$ M^{-1} cm^{-1}) or nitroso-melatonin ($\varepsilon_{345} = 7070$ M^{-1} cm^{-1}) was calculated.

DHR-123. NODTTNO (50 μM) was allowed to react with DHR-123 (50 μM) for 180 min at 37 °C, the concentration of rhodamine-123 was quantified photometrically at $\lambda_{max} = 500$ nm ($\varepsilon_{500} = 78\,000$ M^{-1} cm^{-1}).

DAF-2, APF, HPF. 15 μM NODTTNO were mixed immediately with DAF-2, APF or HPF (10 μM each), and the samples were incubated for 180 min at 37 °C in the dark room. Afterwards, the concentration of DAF-2T or fluorescein was read fluorometrically. The APF- and HPF-derived formation of fluorescein or the DAF-2-mediated formation of DAF-2T were quantified by reading their fluorescence with excitation at 495 nm and emission at 515 nm, respectively. Standard calibration curves were prepared from known amounts of fluorescein and DAF-2T.

Quantum chemical calculations

Complete basis set (CBS-QB3) computations were carried out with the Gaussian 03 (Revision A.11.3) suite of programs.[60] Aqueous solvation free energies were evaluated on the optimized gas-phase geometries with the CPCM[61] procedure incorporated in Gaussian 03. Both the CPCM/UHF/6-31+G(d) and the CBS-QB3 methodology are known to provide estimates within "chemical accuracy" (± 2–3 kcal mol^{-1}). Isotropic absolute shielding constants of the nitrogen nucleus were calculated with the individual gauges for atoms in molecules (IGAIM) protocol[62] at the B97-2/aug-cc-pVDZ level of theory. The optimization of the structure and molecular interactions with the solvent were followed at the same level of theory as described above.

Statistics

All experiments were carried out independently at least three times on different days. The results are expressed as means ± S.D.

Acknowledgements

Sonja Liebeskind was supported by an IFORES grant of the Universität Duisburg-Essen.

References

1 L. J. Ignarro, H. Lipton, J. C. Edwards, W. H. Baricos, H. L. Hyman, P. J. Kadowitz and C. A. Gruetter, *J. Pharmacol. Exp. Ther.*, 1981, **218**, 739–749.
2 S. Moncada, R. M. J. Palmer and E. A. Higgs, *Pharmacol. Rev.*, 1991, **43**, 109–142.
3 J. S. Stamler, *Circ. Res.*, 2004, **94**, 414–417.
4 B. M. Gaston, J. Carver, A. Doctor and L. A. Palmer, *Mol. Interventions*, 2003, **3**, 253–263.
5 S. R. Jaffrey, H. Erdjument-Bromage, C. D. Ferris, P. Tempst and S. H. Snyder, *Nat. Cell Biol.*, 2001, **3**, 193–197.
6 G. Melino, F. Bernassola, R. A. Knight, M. T. Corasaniti, G. Nistico and A. Finazzi-Agro, *Nature*, 1997, **388**, 432–433.
7 J. B. Mannick, X. Q. Miao and J. S. Stamler, *J. Biol. Chem.*, 1997, **272**, 24125–24128.
8 Y.-M. Kim, R. V. Talanian and T. R. Billiar, *J. Biol. Chem.*, 1997, **272**, 31138–31148.
9 S. Z. Lei, Z.-H. Pan, S. K. Aggarwal, H.-S. V. Chen, J. Hartmann, N. J. Sucher and S. A. Lipton, *Neuron*, 1992, **8**, 1987–1099.
10 L. Xu, J. P. Eu, G. Meissner and J. S. Stamler, *Science*, 1998, **279**, 234–237.
11 J. Sun, C. Xin, J. P. Eu, J. S. Stamler and G. Meissner, *Proc. Natl. Acad. Sci. USA*, 2001, **98**, 11158–11162.
12 S. P. Singh, J. S. Wishnok, M. Keshive, W. M. Deen and S. R. Tannenbaum, *Proc. Natl. Acad. Sci. USA*, 1996, **93**, 14428–14433.
13 P. S.-Y. Wong, J. Hyun, J. M. Fukuto, F. N. Shirota, E. G. deMaster, D. W. Shoeman and H. T. Nagasawa, *Biochemistry*, 1998, **37**, 5362–5371.
14 D. A. Stoyanovsky, Y. Y. Tyurina, V. A. Tyurin, D. Anand, D. N. Mandavia, D. Gius, J. Ivanova, B. Pitt, T. R. Billiar and V. E. Kagan, *J. Am. Chem. Soc.*, 2005, **127**, 15815–15823.
15 D. R. Arnelle and J. S. Stamler, *Arch. Biochem. Biophys.*, 1995, **318**, 279–285.
16 C. Petit, P. Hoffmann, J. P. Souchard, F. Nepveu and S. Labidalle, *C. R. Seances Soc. Biol. Ses Fil.*, 1996, **190**, 641–650.
17 J. P. Barton and J. E. Packer, *Int. J. Radiat. Phys. Chem.*, 1970, **2**, 159–166.
18 M. Quintiliani, R. Badiello, M. Tamba, A. Esfandi and G. Gorin, *Int. J. Radiat. Biol.*, 1977, **32**, 195–202.
19 D. Nikitovic and A. Holmgren, *J. Biol. Chem.*, 1996, **271**, 19180–19185.
20 A. P. Dicks, H. R. Swift, D. L. H. Williams, A. R. Butler, H. H. Al-Sa'doni and B. G. Cox, *J. Chem. Soc., Perkin Trans. 2*, 1996, 481–487.
21 D. L. H. Williams, *Chem. Commun.*, 1996, 1085–1091.
22 M. W. Brock, C. Mathes and W. F. Gilly, *J. Gen. Physiol.*, 2001, **118**, 113–133.
23 S. Goldstein and G. Czapski, *J. Am. Chem. Soc.*, 1996, **118**, 3419–3425.
24 M. Kirsch and H. de Groot, *J. Biol. Chem.*, 2002, **277**, 13379–13388.
25 N. W. Kooy, J. A. Royall, H. Ischiropoulos and J. S. Beckman, *Free Radical Biol. Med.*, 1994, **16**, 149–156.
26 H. Ischiropoulos, D. Duran and J. Horwitz, *J. Neurochem.*, 1995, **65**, 2366–2372.
27 M. Kirsch, A. Fuchs and H. de Groot, *J. Biol. Chem.*, 2003, **278**, 11931–11936.
28 K. M. Miranda, M. G. Espey, N. Ludwick, S. M. Kim, D. Jourd'heuil, M. B. Grisham, M. Feelisch, J. M. Fukuto and D. A. Wink, *J. Biol. Chem.*, 2001, **276**, 1720–1727.
29 K. Setsukinai, Y. Urano, K. Kakinuma, H. J. Majima and T. Nagano, *J. Biol. Chem.*, 2003, **278**, 3170–3175.
30 R. S. Lewis, S. R. Tannenbaum and W. D. Deen, *J. Am. Chem. Soc.*, 1995, **117**, 3933–3939.
31 D. A. Stoyanovsky, R. Clancy and A. I. Cederbaum, *J. Am. Chem. Soc.*, 1999, **121**, 5093–5094.
32 L. Grossi and P. C. Montevecchi, *Chem.–Eur. J.*, 2002, **8**, 380–387.
33 K. Sonnenschein, H. de Groot and M. Kirsch, *J. Biol. Chem.*, 2004, **279**, 45433–45440.
34 M. A. Marti, S. E. Bari, D. A. Estrin and F. Doctorovich, *J. Am. Chem. Soc.*, 2005, **127**, 4680–4684.
35 K. M. Faulkner, S. I. Liochev and I. Fridovich, *J. Biol. Chem.*, 1994, **269**, 23471–23476.
36 M. Kirsch and H. de Groot, *J. Pineal Res.*, 2008, **44**, 244–249.
37 S. I. Liochev and I. Fridovich, *J. Biol. Chem.*, 2001, **276**, 35253–35257.
38 M. Kelm, R. Dahmann, D. Wink and M. Feelisch, *J. Biol. Chem.*, 1997, **272**, 9922–9932.
39 B. Bujnicki, J. Drabowicz, M. Mikolajczyk, A. Kolbe and L. Stefaniak, *J. Org. Chem.*, 1996, **61**, 7593–7596.
40 L. Stefaniak, G. A. Webb and M. Witanowski, *Annu. Rep. NMR Spectrosc.*, 1993, **25**.
41 S. Goldstein and G. Czapski, *J. Am. Chem. Soc.*, 1995, **117**, 12078–12084.
42 D. L. H. Williams, *Nitrosation reactions and the chemistry of nitric oxide*, Elsevier, Amsterdam, 2004.
43 L. J. Ignarro, J. M. Fukuto, J. M. Griscavage, N. E. Rogers and R. E. Byrns, *Proc. Natl. Acad. Sci. USA*, 1993, **90**, 8103–8107.
44 P. G. Wang, M. Xian, X. Tang, X. Wu, Z. Wen, T. Cai and A. J. Janczuk, *Chem. Rev.*, 2002, **102**, 1091–1134.
45 M. D. Bartberger, J. D. Mannion, S. C. Powell, J. S. Stamler, K. N. Houk and E. J. Toone, *J. Am. Chem. Soc.*, 2001, **123**, 8868–8869.
46 M. Tronc, A. Huetz, M. Landau, F. Pichou and J. Reinhardt, *J. Phys. B: At. Mol. Phys.*, 1975, **8**, 1160–1169 .
47 V. Shafirovich and S. V. Lymar, *Proc. Natl. Acad. Sci. USA*, 2002, **99**, 7340–7345.
48 D. A. Stoyanovsky, *J. Am. Chem. Soc.*, 2005, **127**, 15815–15823.
49 Y. Zhang and N. Hogg, *Free Radical Biol. Med.*, 2005, **38**, 831–838.
50 A. Meister, *J. Biol. Chem.*, 1988, **263**, 17205–17208.
51 R. K. Murray, D. K. Granner, P. A. Mayes and V. W. Rodwell, *Harper's Illustrated Biochemistry*, McGraw-Hill Companies, New York, 24th edn, 2003.
52 M. Kirsch and H. de Groot, *J. Biol. Chem.*, 2000, **275**, 16702–16708.
53 M. Kirsch and H. de Groot, *J. Pineal Res.*, 2006, **40**, 10–17.
54 A. J. Holmes and D. L. H. Williams, *J. Chem. Soc., Perkin Trans. 2*, 2000, 1639–1644.
55 R. Bonnett and R. Holleyhead, *J. Chem. Soc., Perkin Trans. 1*, 1974, 962–964.

56 G. L. Ellmann, *Arch. Biochem. Biophys.*, 1958, **74**, 443.
57 G. L. Ellmann, *Arch. Biochem. Biophys.*, 1958, **74**, 443–450.
58 H. U. Bergmeyer, M. Grassl and H.-E. Walter, in *Methods of Enzymatic Analysis*, ed. H. U. Bergmeyer, Verlag Chemie, Weinheim, 1983, vol. II, p. 165.
59 I. Ioannidis and H. de Groot, *Biochem. J.*, 1993, **296**, 341–345.
60 M. J. Frisch, G. W. Trucks, H. B. Schlegel, P. M. W. Gill, B. G. Johnson, M. A. Robb, J. R. Cheeseman, T. Keith, G. A. Petersson, J. A. Montgomery, K. Raghavachari, M. A. Al-Laham, V. G. Zakrzewski, J. V. Ortiz, J. B. Foresman, J. J. Cioslowski, B. B. Stefanov, A. Nanayakkara, M. Challacombe, C. Y. Peng, P. Y. Ayala, W. Chen, M. W. Wong, J. L. Andres, E. S. Replogle, R. Gomperts, R. L. Martin, D. J. Fox, J. S. Binkley, D. J. Defrees, J. Baker, J. P. Stewart, M. Head-Gordon, C. Gonzalez and J. A. Pople, *Gaussian 98W*, Gaussian Inc., Pittsburgh, PA, Revision A.9 edn, 2000.
61 V. Barone, M. Cossi and J. Tomasi, *J. Chem. Phys.*, 1997, **107**, 3210–3221.
62 T. Gregor, F. Mauri and R. Car, *J. Chem. Phys.*, 1999, **111**, 1815–1822.